

# Contents lists available at ScienceDirect

# Polymer

journal homepage: www.elsevier.com/locate/polymer





# Crystallization kinetics and equilibrium melting temperature of poly(ether ketone ketone) with high terephthalate content utilizing fast scanning calorimetry

Michelle E. Pomatto a, Robert B. Moore a,b,\*

- <sup>a</sup> Macromolecules Innovation Institute, Virginia Tech, Blacksburg, VA, 24061, United States
- Department of Chemistry, Virginia Tech, Blacksburg, VA, 24061, United States

#### ABSTRACT

Fast scanning calorimetry (FSC) was used to analyze the crystallization kinetics and determine the equilibrium melting temperature ( $T_m^0$ ) of KEPSTAN PEKK 8001 (PEKK 80/20) with a terephthalate to isophthalate (T/I) ratio of 80/20. Quantitative  $^1H$ , qualitative  $^{13}C$  and 2D HSQC NMR spectroscopy for KEPSTAN 8001 and KEPSTAN 7002 were collected to confirm linear topology and comonomer composition. Utilizing FSC, the isothermal crystallization kinetics for PEKK 80/20 are reported for the first time over a large temperature range from 200 °C to 310 °C utilizing an interrupted isothermal crystallization method. The crystallization kinetics of PEKK 80/20 exhibits parabolic behavior with the most rapid crystallization occurring at 260 °C. Compared to earlier studies of PEKK copolymers with lower T/I ratios (i.e., PEKK 70/30 and 60/40) using conventional DSC, PEKK 80/20 is observed to crystallize up to 1 to 2 orders of magnitude faster (i.e., at rates inaccessible with conventional DSC). The  $T_m^0$  of PEKK 80/20 was determined utilizing the zero-entropy-production temperature ( $T_{ZEP}$ ) allowing for the first time an accurate determination of the equilibrium melting temperature of 382 °C. This value was compared to a traditional Hoffman-Weeks linear extrapolation over a range of heating rates (500 K/s – 20,000 K/s) to arrest melt-reorganization upon heating. Due to unavoidable crystalline reorganization during slow heating scans with conventional DSC, this new value for  $T_m^0$  using FSC is significantly higher than the commonly referenced literature value of 368 °C. The double melting peak behavior observed after isothermal crystallization of PEKK 80/20 is discussed and understood to be due to reorganization during heating at relatively slow heating rates, as commonly observed with conventional DSC.

# 1. Introduction

Poly(aryl ether ketone)s (PAEKs) are a family of thermoplastics widely used in industrial sectors including aerospace, automotive, and oil and gas industries due to their excellent mechanical performance and chemical resistance properties. One interesting PAEK, poly(ether ketone ketone) (PEKK) is a linear semi-crystalline thermoplastic gaining increased interest due to excellent properties including high impact strength, chemical resistance, high glass transition and melting temperatures, low flammability, and good processibility [1-3]. PEKK is of particular interest due to the ability to tune the melting and glass transition temperatures by tuning the ratio of terephthalate to isophthalate moieties when synthesized [4]. This ratio is termed the "T/I ratio" and can be seen in the molecular structure of PEKK shown in Fig. 1. The isophthalate containing monomers produce a configurational defect within the chain structure, which lowers crystallizability leading to a reduction in melting temperature and crystallization rate with increasing isophthalate content. The isophthalate "kink" also leads to an increase in chain mobility attributed to greater free volume, and thus a

reduction in the glass transition temperature [4,5]. Therefore, a deeper understanding of the effect of T/I ratio on melting and glass transition temperature is important for industrial applications as accurate knowledge of the thermo-physical properties greatly influences processibility and final properties for semi-crystalline polymers such as PEKK.

It is known that thermal processing conditions influence crystallization behavior. One interesting phenomenon arising from variable thermal histories is multiple melting peaks, observed in many polymers including polyethylene terephthalate (PET) [6,7], isotactic polystyrene [8], bisphenol-A polycarbonate [9], ethylene/1-octane copolymer [10], poly(ether ether ketone) (PEEK) [11–14] and PEKK [1,4,5,15,16]. The origin of multiple melting peaks can be attributed to several reasons: (1) different crystal structures (i.e., polymorphism), each with a different melting temperature, (2) the melting of small secondary lamella between primary lamella whereby small secondary lamella melt at a lower temperature than the primary lamella (i.e., bimodal melting), or (3) melt and rapid reorganization whereby small thin crystals melt at a lower temperature during heating and rapidly recrystallize into thicker lamella that subsequently melt at a higher temperature (i.e.,

<sup>\*</sup> Corresponding author. Macromolecules Innovation Institute, Virginia Tech, Blacksburg, VA, 24061, United States. *E-mail address:* rbmoore3@vt.edu (R.B. Moore).

**Fig. 1.** Molecular structure of poly(ether ketone ketone) copolymer repeat unit comprising of terephthaloyl, "T" and isophthaloyl, "T" isomers. X=80 and Y=20 for PEKK 80/20.

melt-reorganization). Isothermal crystallization kinetic studies of PEKK 60/40 [1,4,17] and PEKK 70/30 [1] from the melt have shown an additional endotherm during melting which occurs about 10  $^{\circ}\mathrm{C}$  above the isothermal annealing temperature. Only one crystal form is observed for PEKK when crystallized from the melt [18] and so this multiple melting peak behavior has been attributed to bimodal melting. However, studies exploring the effect of heating rate on the multiple melting peak behavior have not been performed for PEKK, and so multiple melting peak behavior due to the melt-reorganization of crystals cannot be ruled out.

The effect of heating rate on the multiple melting peak behavior has been explored in a similar polyaryl ether ketone, PEEK. Marand et al. [11] found that the multiple melting peak behavior observed in PEEK was dependent on the heating rate, which suggested that the low temperature melting peak is due to melting of small secondary crystals. Furushima et al. [19] suggested the reorganization during heating was not fully suppressed due to the slow heating rate of the conventional DSC used by Marand. This led to further exploration of the bimodal melting behavior dependence on the heating rate of isothermally crystallized PEEK [19] and polyamide 6 [20] where the reorganization upon heating of the two crystal populations with different melting kinetics were suppressed using fast scanning differential calorimetry (FSC). Tardif et al. [21] utilized FSC to determine the crystallization kinetics of isothermally crystallized PEEK and observed a shifting of the higher endothermic peak to a lower melting temperature with increasing heating rate while the lower endothermic peak shifted to higher temperatures with faster heating rates, leading to a single melting peak observed at heating rates of 2,000 K/s. It was concluded that these observations were evidence that the multiple melting peak behavior is due to the melting and recrystallization of crystallites upon heating. Furushima et al. further showed that with increased heating rate (500 K/s to 60,000 K/s), the bimodal melting peaks of isothermally crystallized PEEK at high degrees of crystallinity converged to one peak and then exhibited bimodal character again at heating rates above 20,000K/s [19]. They suggested this disappearance of bimodal melting is due to reorganization of secondary crystallites being suppressed with faster heating and the true melting of the primary and secondary crystallites being observed at faster heating rates. Real time small angle X-ray scattering supports the existence of two distinct populations of crystal thicknesses for isothermally crystallized PEEK [22].

The crystallization kinetics [4,5,17] and equilibrium melting temperature ( $T_m^o$ ) [5] of PEKK has been explored by various groups with a primary focus on PEKK 60/40 and 70/30. The crystallization kinetics of PEKK 80/20 is less explored most likely due to its very fast-crystallizing nature and the limitations of standard DSC heating rates to accurately observe the isothermal crystallization of PEKK 80/20. Most notably, Gardner et al. [4] synthesized a set of PEKK 80/20 samples and attempted to quantify the crystallization half time ( $t_{1/2}$ ) and  $T_m^o$  using conventional DSC. The values they reported are most commonly referenced in recent literature [23,24]. We have now identified a number of improvements in methodology to allow for more accurate analysis of the crystallization kinetics and determination of the  $T_m^o$  for PEKK 80/20. The first improvement in methodology is utilization of a commercially available material, KEPSTAN PEKK systems manufactured by Arkema,

instead of a lab grade material. The TGA of the PEKK 80/20 lab sample showed thermal degradation as early as 400  $^{\circ}\text{C}$ , adding to the fact that the sample analyzed by Gardner et al. is not translatable to current commercially available PEKK 80/20 with a degradation temperature of 600  $^{\circ}\text{C}$  (see below).

The second improvement in methodology is the use of FSC for true isothermal crystallization analysis of fast crystallizing materials, such as PEKK 80/20. Recent advances in FSC offer heating and cooling rates that are many orders of magnitude faster than standard DSC. For example, the quench rate of 320 K/min (5.3 K/s) used in the Gardner analysis of PEKK 80/20 is significantly slower than the critical quench rate to prevent crystallization upon cooling from the melt (see below). Arresting crystallization upon cooling from the melt is critical to ensure true isothermal crystallization and prevention of annealing of crystals, leading to an improper value of  $T_{\rm m}^{\rm o}$  [25].

The third improvement in methodology is the enhancement of the Hoffman-Weeks linear extrapolation methodology to determine T<sub>m</sub>. In this work, two different methods of determining T<sub>m</sub><sup>0</sup> are performed and compared. The first being a linear Hoffman-Weeks extrapolation of the zero-entropy-production melting temperature (T<sub>ZEP</sub>) versus the isothermal crystallization temperature (Tiso). Recently, this approach has been examined in the literature [20,26-28] and is considered to be the more accurate method, as T<sub>ZEP</sub> represents the melting point of the examined crystals without non-equilibrium effects of reorganization, recrystallization, and superheating [29]. The second method is a linear Hoffman-Weeks extrapolation of the peak melting temperature (T<sub>m,peak</sub>) versus Tiso at sufficiently fast heating rates to prevent reorganization. Thoroughly examined by Marand et al., the conditions under which the linear Hoffman-Weeks extrapolation provides a reliable estimate of the T<sub>m</sub> include minimizing isothermal thickening by limiting the degree of crystallinity of chain folded crystals. Chain folded crystals of limited degree of crystallinity are known to exhibit a relatively narrow distribution of thicknesses [25,30,31]. It has even been demonstrated that different equilibrium melting temperatures are reported for identical samples that differ only by degree of crystallinity [32]. Gardner et al. described a 30 min isothermal crystallization period during their method of T<sub>m</sub><sup>0</sup> determination. This isothermal crystallization period is lengthy compared to the crystallization kinetics of PEKK 80/20, and so it is likely that the degree of crystallinity of the samples was near maximum. As previously discussed, this will lead to an improper extrapolation of the T<sub>m</sub><sup>o</sup>, as the peak melting temperature is known to shift to higher temperatures with increased isothermal crystallization time [25].

Due to these identified improvements, it is clear that a refined measurement of the crystallization kinetics and T<sub>m</sub> of PEKK 80/20 utilizing FSC is necessary to accurately determine these material parameters utilizing state-of-the-art methodologies for the commercially available KEPSTAN PEKK 8001. The purpose of this work is to utilize FSC to evaluate the crystallization kinetics of PEKK 80/20 over a large temperature range and make use of refined measurement methodologies to determine a representative equilibrium melting temperature for KEPSTAN PEKK 8001. This includes the collection of NMR spectra of PEKK 80/20 and 70/30 to verify linear topology and T/I ratio. This study identifies the necessity of the rapid scanning capabilities of FSC to properly evaluate the crystallization kinetics of PEKK 80/20 and elucidate the origin of multiple melting endotherms observed after isothermal crystallization. Additionally, this study includes a detailed analysis and discussion of the multiple melting peak behavior of PEKK 80/20 at low heating rates due to melt-reorganization. Furthermore, a quantitative analysis supporting this conclusion which utilizes the zeroentropy-production temperature is discussed. Finally, the T<sub>m</sub> of PEKK 80/20 is determined utilizing state-of-the-art methodologies.

## 2. Experimental

#### 2.1. Materials

Poly(ether ketone ketone) pellets, KEPSTAN® 7002 (vendor reported T/I = 70/30,  $T_m = 331\,^\circ\text{C},\,T_g = 162\,^\circ\text{C},\,\text{MFR}$  at  $380\,^\circ\text{C}/5$  kg =  $35\,\text{cm}^3/10$  min) and KEPSTAN® 8001 (vendor reported T/I =  $80/20,\,T_m = 358\,^\circ\text{C},\,T_g = 165\,^\circ\text{C},\,\text{MFR}$  at  $380\,^\circ\text{C}/5$  kg =  $15\,\text{cm}^3/10$  min) were obtained from Arkema and referenced herein as PEKK 70/30 and PEKK 80/20, respectively. Pellets were washed with acetone and deionized water and dried at  $80\,^\circ\text{C}$  in a vacuum oven for 8 h prior to use. Dichloroacetic acid (DCA) was purchased from Sigma-Aldrich and used as received.

#### 2.2. NMR spectroscopy

The T/I comonomer ratios and linear topology of PEKK 70/30 and PEKK 80/20 were verified by <sup>1</sup>H NMR spectroscopy at room temperature in DCA and deuterated chloroform (CDCl<sub>3</sub>) with 0.05% v/v TMS on a Bruker Avance 400 MHz spectrometer. Spectra were collected as the average of 128 scans with relaxation delay of 10 s. The PEKK samples were dissolved in DCA at 185 °C to a concentration of 10% w/v. Once dissolved, the solution was cooled to room temperature and diluted with CDCl<sub>3</sub> with 0.05% v/v TMS to a concentration of 5% w/v. The solvent system was previously reported [33] from work with the similar poly (aryl ether ketone), PEEK. The <sup>1</sup>H NMR splitting patterns are designated as follows: s (singlet), d (doublet), dd (double doublet), t (triplet), and m (multiplet). Qualitative <sup>13</sup>C NMR spectra were measured using a Bruker Avance 500 MHz spectrometer. The PEKK samples were prepared following the same procedure as described previously to a final concentration of 10% w/v. Spectra were collected as the average of 256 scans with relaxation delay of 2 s. 2D heteronuclear correlation spectroscopy (HSQC) was collected on an Agilent U4-DD2 400 MHz spectrometer. The PEKK samples were prepared following the procedure as described previously.

#### 2.3. Thermogravimetric analysis

A TA Instruments TGA Q500 was used to evaluate the thermal stability of PEKK 80/20 to verify no degradation occurs during FSC analysis (Fig. S1). Samples were prepared by melt pressing at 400  $^{\circ}\text{C}$  and quenched in ice water. The amorphous films were dried at 80  $^{\circ}\text{C}$  in a vacuum oven overnight before use. All analyses were performed with a ramp rate of 20  $^{\circ}\text{C/min}$  in nitrogen.

# 2.4. Fast scanning chip calorimetry

A Mettler Toledo Flash DSC 1 with a Huber intra cooler TC100 was employed to analyze the crystallization behavior of PEKK 80/20. Prior to any evaluation, the chip sensors were individually conditioned and temperature corrected utilizing Mettler Toledo supplied calibration data and following Mettler Toledo instrument specifications. The temperature was experimentally calibrated by an indium standard for each heating rate. The onset of indium melting versus heating rate was used to determine the corrected horizontal shifts of the experimental melting profiles. All experiments were conducted in an ultra-high purity N2 gas environment with a flow rate of 60 mL/min to limit oxidation and moisture in the sample chamber. Amorphous PEKK samples were prepared by melt pressing at 400 °C, a temperature significantly above any reported T<sub>m</sub><sup>o</sup> and below the degradation temperature of PEKK 80/20, to a thickness of 0.025 mm and melt-quenched in ice water followed by drying in a vacuum oven overnight at 80  $^{\circ}\text{C}.$  Thin samples for FSC measurements were cut by microtome (2  $\mu m$  thickness) from the amorphous film and laterally cut to size by scalpel under a microscope. A thin layer of Wacker AK 60000 silicone oil was spread on the sensor prior to sample placement to improve thermal contact and allow for removal of sample after testing. All samples were pre-melted at 5 K/s to

 $400~^{\circ}\text{C}$  for 1 s to establish good thermal contact. The sample mass was estimated from the change in heat capacity at the glass transition temperature from an amorphous sample with all samples measured between 4 ng - 13 ng. Experiments were repeated with fresh samples and over multiple chip sensors to ensure reproducibility.

To prevent crystallization upon cooling, the critical cooling rate from the melt was determined utilizing rapid cooling rates as shown in the time-temperature profile in Fig. S2 and found to be 10 K/s for PEKK 80/20 (Fig. S3). A cooling rate of 500 K/s was utilized for all experiments. The time in the melt to completely remove thermal history was determined utilizing the time-temperature profile in Fig. S4. The minimum time required to remove thermal history at 400  $^{\circ}$ C was found to be 0.1 s for PEKK 80/20 (Fig. S5). A melt time of 1 s was utilized for all experiments.

The crystallization kinetics for PEKK 70/30 and PEKK 80/20 were analyzed utilizing an interrupted isothermal crystallization (IIC) method [21,34]. The time temperature profile for the IIC method is shown in Fig. 2. The isothermal crystallization temperatures (T<sub>iso</sub>) between 200 °C to 310 °C were analyzed by this method. After removing thermal history at 400 °C for a minimum of 1 s, the sample was quenched at 500 K/s to the respective  $T_{iso}$  and held for varying amounts of time (0.1 s – 12,000 s). The sample was quenched at -500 K/s to below the  $T_{\rm g}$  to arrest any further crystallization. The partially crystallized sample was then heated to 400 °C at a heating rate of 500 K/s to measure degree of crystallinity as observed by the integration of the melting endotherm upon heating. The maximum isothermal crystallization time (tiso) was determined when the melting enthalpy remained at a constant value with increasing tiso. Fig. S6 demonstrates an example of a change in melting enthalpy with increasing  $t_{iso}$  for PEKK 80/20 at a  $T_{iso}$  of 260 °C. The maximum isothermal crystallization time is dependent on Tiso. The observed melting enthalpy versus tiso was used to calculate crystallization half-time (t<sub>1/2</sub>) for PEKK 80/20 over a range of isothermal crystallization temperatures.

# 2.5. Equilibrium melting temperature

The equilibrium melting temperature  $(T_m^o)$  of PEKK 80/20 was analyzed utilizing two different methods: 1) the linear Hoffman-Weeks extrapolation of the zero-entropy-production temperature  $(T_{ZEP})$  of isothermally crystallized samples with minimal crystal thickening and 2) the linear Hoffman-Weeks extrapolation of the peak melting temperature  $(T_{m,peak})$  of isothermally crystallized samples with minimal crystal thickening. The time-temperature profile utilized to perform both of the Hoffman-Weeks extrapolations of PEKK 80/20 is shown in

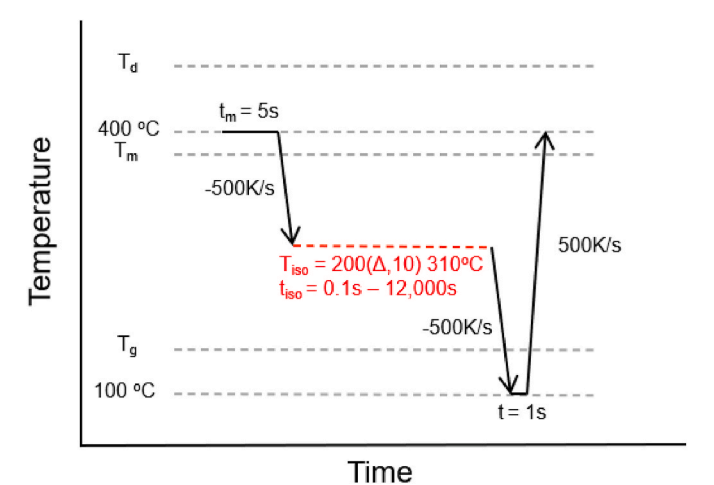


Fig. 2. Time-temperature profile for the Flash DSC interrupted isothermal crystallization (IIC) method used to determine the  $t_{1/2}$  of PEKK 80/20 and PEKK 70/30 at each  $T_{\rm iso}$ .

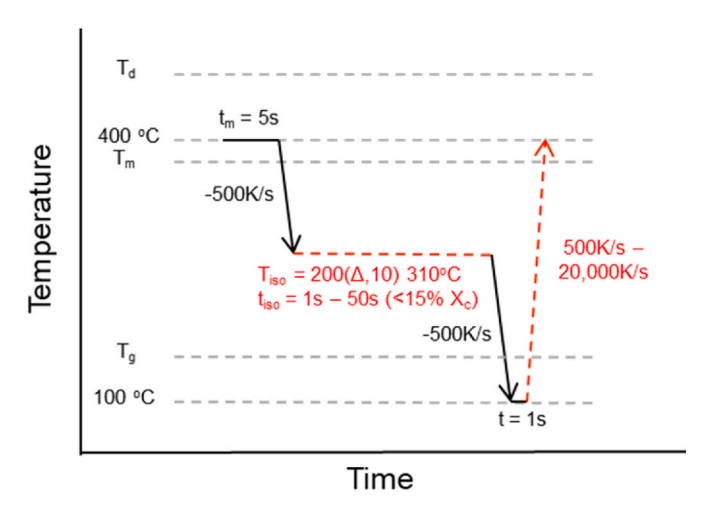


Fig. 3. Time-temperature profile utilized on the Flash DSC for the Hoffman-Weeks analysis of PEKK 80/20.

Fig. 3. After removing thermal history at 400 °C for 1 s, the sample was quenched at 500 K/s to the respective T<sub>iso</sub> and held for varying amounts of time (1 s - 50 s) to allow for low amounts of crystallinity. Utilizing the crystallization kinetics information from the IIC method described previously, it was possible to determine the  $t_{\text{iso}}$  needed to crystalize PEKK 80/20 to a low degree of crystallinity (<15%) at a given  $T_{\rm iso}$ . The sample was then quenched at -500 K/s to below the  $T_g$  to arrest any further crystallization. The partially crystallized sample was then heated to 400 °C at various heating rates to determine the minimum rate needed to eliminate reorganization upon heating for proper HW analysis (see below). For method 1, the peak melting temperature as a function of heating rate was used to determine the TZEP for each Tiso (discussed below). The  $T_{\text{ZEP}}$  values were then plotted as a function of  $T_{\text{iso}}$  to determine the  $T_{m}^{o}$ . For method 2, the peak melting temperature  $(T_{m,peak})$ as a function of T<sub>iso</sub> for each heating rate was then plotted to determine the T<sub>m</sub><sup>0</sup>. The melting peaks were deconvoluted in OriginPro (OriginLab) to extract the peak melting temperature.

#### 3. Results and discussion

## 3.1. NMR of PEKK 80/20 and 70/30

The comonomer content (i.e., T/I ratio) and linear topology of PEKK 70/30 and PEKK 80/20 were verified by NMR. Due to limited solubility of PEKK no NMR characterization of KEPSTAN® PEKK 7002 and KEP-STAN® PEKK 8001 have been reported. We recently discovered dichloroacetic acid (DCA) to be a reasonable solvent for NMR analysis of PAEKs [35]. The aromatic region of the <sup>1</sup>H NMR spectra, peak assignments, and integrations for PEKK 70/30 and PEKK 80/20 are shown in Fig. 4. Both PEKK 70/30 and PEKK 80/20 exhibit proton resonances at 7.19-7.22 (m), 7.68-7.72 (t), 7.90-7.94 (m), 8.04-8.06 (m), and 8.16 (s) ppm associated with the aromatic protons of the terephthalic and isophthalic moieties. The T/I ratio can be determined through comparison of the ratio of the integration of resonance peaks associated with protons labeled 3 or 4, located on the isophthalic monomer unit, to proton 1, located on both the isophthalic and terephthalic units in equal amounts (4 in each unit) for a total value of 4 regardless of the T/I ratio. For simplification, the following equation utilizes the integration of proton 1 equal to 4.

When setting the integration value of  $H_1$  equal to 4, then:

$$x = 1 - \int H_{3 \text{ or } 4}$$
 [1]

Where  $\int H_{\#}$  is the integration of the corresponding resonance peak in Fig. 4, x is the fraction of "T" monomers, y is the fraction of "T" monomers and x+y=1. The number of  $H_1$  protons will not change due to the fact both the T and I monomers contain 4  $H_1$  protons each and the value of T+I will never change. Table 1 shows the range of calculated ratios of

 $\begin{tabular}{ll} \textbf{Table 1} \\ \textbf{Theoretical and calculated T/I ratios utilizing the integration values of protons 3} \\ \textbf{and 4 shown in Fig. 4}. \\ \end{tabular}$ 

Theoretical Ratio "T/I"	Calculated Ratio	
	$\int H_3$	$\int H_4$
70/30	70.5/29.5	71.0/29.0
80/20	80.0/20.0	78.5/21.5

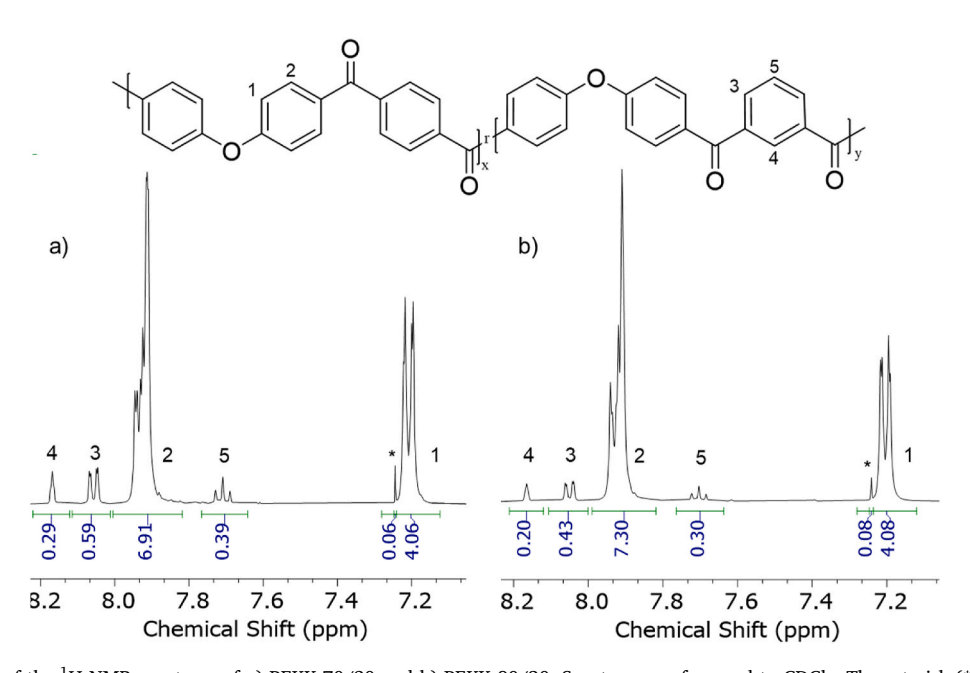


Fig. 4. Aromatic region of the <sup>1</sup>H NMR spectrum of a) PEKK 70/30 and b) PEKK 80/20. Spectra are referenced to CDCl<sub>3</sub>. The asterisk (\*) refers to reference solvent resonance.

PEKK 70/30 and PEKK 80/20 when setting the integration value of proton 1 equal to 4 and utilizing the resultant integration values of protons 3 or 4.

The T/I ratios for PEKK 70/30 and PEKK 80/20 were calculated according to equation (1) utilizing the integration values shown in Fig. 4 and found to range between 70.5/29.5 to 71.0/29.0 and 80.0/20.0 to 78.5/21.5, respectively. These values thus verify the manufacturer's reported T/I ratios for the KEPSTAN® PEKK 7002 (T/I = 70/30) and KEPSTAN® PEKK 8001 (T/I = 80/20) copolymers. Additionally, all resonance peaks in the aromatic region of the  $^1\mathrm{H}$  NMR spectra are accounted for, and no additional peaks appeared in the downfield region which would be associated with branching [36], thus verifying a linear topology. Verifying the linear topology of the polymer is important as the topology of a polymer greatly influences the resultant crystallization kinetics.

Qualitative  $^{13}$ C NMR spectroscopy was also used to further verify the peak assignments of PEKK 70/30 and PEKK 80/20. The  $^{13}$ C NMR spectra for PEKK 70/30 and PEKK 80/20 are shown in Fig. 5. PEKK 70/30 and PEKK 80/20 exhibit distinct  $^{13}$ C resonances at 197, 160, 140, 137, 134, 133, 131, 130, 129, and 119 ppm associated with the  $^{13}$ C resonance of the terephthalic and isophthalic moieties. Peak correlations between the  $^{14}$ H and  $^{13}$ C spectra (i.e., 2D NMR) were probed by a heteronuclear single quantum coherence (HSQC) correlation experiment to verify the peak assignments (see Fig. S7).

#### 3.2. Isothermal crystallization kinetics of PEKK 80/20

The crystallization process for PEKK 80/20 is too fast to analyze by standard DSC but too slow for direct isothermal analysis with Flash DSC. Consequently, the crystallization kinetics were analyzed utilizing the previously described IIC method. This method utilizes the melting enthalpy upon heating after isothermal crystallization to calculate the degree of crystallinity instead of a direct measure of heat flow during the isothermal crystallization process [21,34]. The fractional crystallinity ( $\Phi$ ) of PEKK 80/20 as a function of time at the designated crystallization temperature,  $T_{\rm iso}$ , was recorded and further discussed in Fig. S8.

The crystallization half-time,  $t_{1/2}$ , of PEKK 80/20, or time when the fractional crystallinity reaches 50% of total crystallizable content (i.e.,  $\Phi=0.5$ ) was extracted from Fig. S8 and plotted in Fig. 6 as a function of the isothermal crystallization temperature,  $T_{iso}$ . To confirm accuracy of the IIC method, the  $t_{1/2}$  of PEKK 70/30 isothermally crystallized at 210,

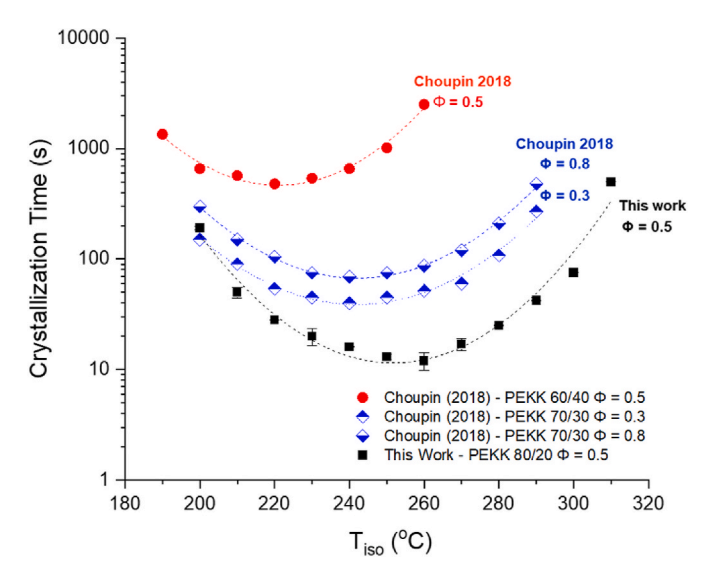


Fig. 6. The fractional crystallinity curves for PEKK 80/20 (black, square) determined in this work, and 70/30 [37] (blue diamond), and 60/40 [37] (red circle), determined by Choupin (2018). Fractional crystallinity of each data set indicated by  $\Phi$ . Dashed lines to guide the eye only. (For interpretation of the references to colour in this figure legend, the reader is referred to the Web version of this article.)

230, 240, 250, 260 and 280 °C were also collected and compared to literature [37] (Fig. S9). For PEKK 80/20 the crystallization kinetics are fastest at 260 °C ( $t_{1/2}=12~s$ ) due to the balance of nucleation and diffusion-controlled crystallization with limits between the  $T_g$  and  $T_m^0$ . Comparison of the  $t_{1/2}$  performed in this work to the kinetics of PEKK 70/30 and 60/40 performed by Choupin et al. follows the expected trend with a decrease in  $t_{1/2}$  and increase in ideal  $T_{iso}$  (at minimum  $t_{1/2}$ ) with an increase in T/I ratio. Increasing kinetics with an increase in terephthalate content is well understood and explained by a decrease in isophthalate content corresponding to an increase in pristine crystallizable terephthalate chain segments and the isophthalate monomers acting as structural defects, resulting in slower crystallization kinetics and decreased crystalline phase compactness [4,17].

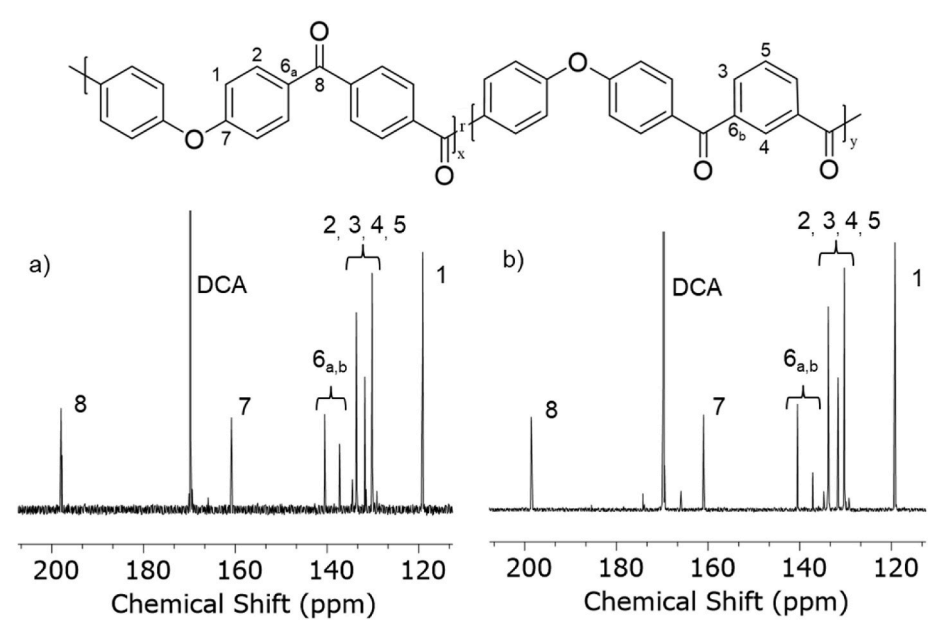


Fig. 5. 13C NMR spectra of a) PEKK 70/30 and b) PEKK 80/20. Spectra are recorded in DCA/CDCl<sub>3</sub> at 25 °C. Referenced to CDCl<sub>3</sub>.

#### 3.3. Equilibrium melting temperature determination

Commonly referenced literature reports the equilibrium melting temperature,  $T_m^{\rm o}$ , of PEKK 80/20 as 368 °C [4]. As previously discussed, the need to determine a more representative equilibrium melting temperature for PEKK 80/20, with an updated methodology, is established as: (1) the reported  $T_m^{\rm o}$  is for a lab grade material and not a commercially available material (KEPSTAN® PEKK 8001), (2) a controlled quench rate for true isothermal crystallization was not attainable with instrumentation available at that time, and (3) the experimentally measured melting behavior used to create the Hoffman-Weeks plot was not free from crystal reorganization and thickening during annealing, which is known to lead to an inaccurate value of  $T_m^{\rm o}$  (see Figs. S10 and S11).

Another complication with the melting behavior of PEKK arises from the multiple melting peak behavior likely due to reorganization upon heating, as observed in the similar poly(aryl ether ketone), PEEK [19]. This reorganization upon heating will influence the peak melting

temperature and therefore lead to invalid T<sub>m</sub> analysis by linear Hoffman-Weeks extrapolation utilizing the peak melting temperatures. To identify if the multiple melting peak behavior is due to melt-reorganization upon heating, the melting behavior of PEKK 80/20 as a function of heating rate was analyzed. Utilizing the fractional crystallinity data in Fig. S8, PEKK 80/20 was crystallized to low degrees of crystallinity (<15%) at specific  $T_{iso}$  and the melting behavior as a function of heating rate was observed. As discussed previously, it is known that large amounts of crystallinity lead to an improper extrapolation of the  $T_{\text{m}}^{\text{o}}\text{,}$  as the peak melting temperature is known to shift to higher melting temperatures with increased annealing time (i.e., attributed to lamellar thickening at longer tiso) [25]. In Fig. S6 a clear example of the shifting of the peak melting temperature is seen for PEKK 80/20 isothermally crystallized at 260 °C for various amounts of time is observed. This result supports the necessity for isothermally crystallizing to low degrees of crystallinity (short t<sub>iso</sub>) for proper T<sub>m</sub><sup>o</sup> analysis of PEKK 80/20.

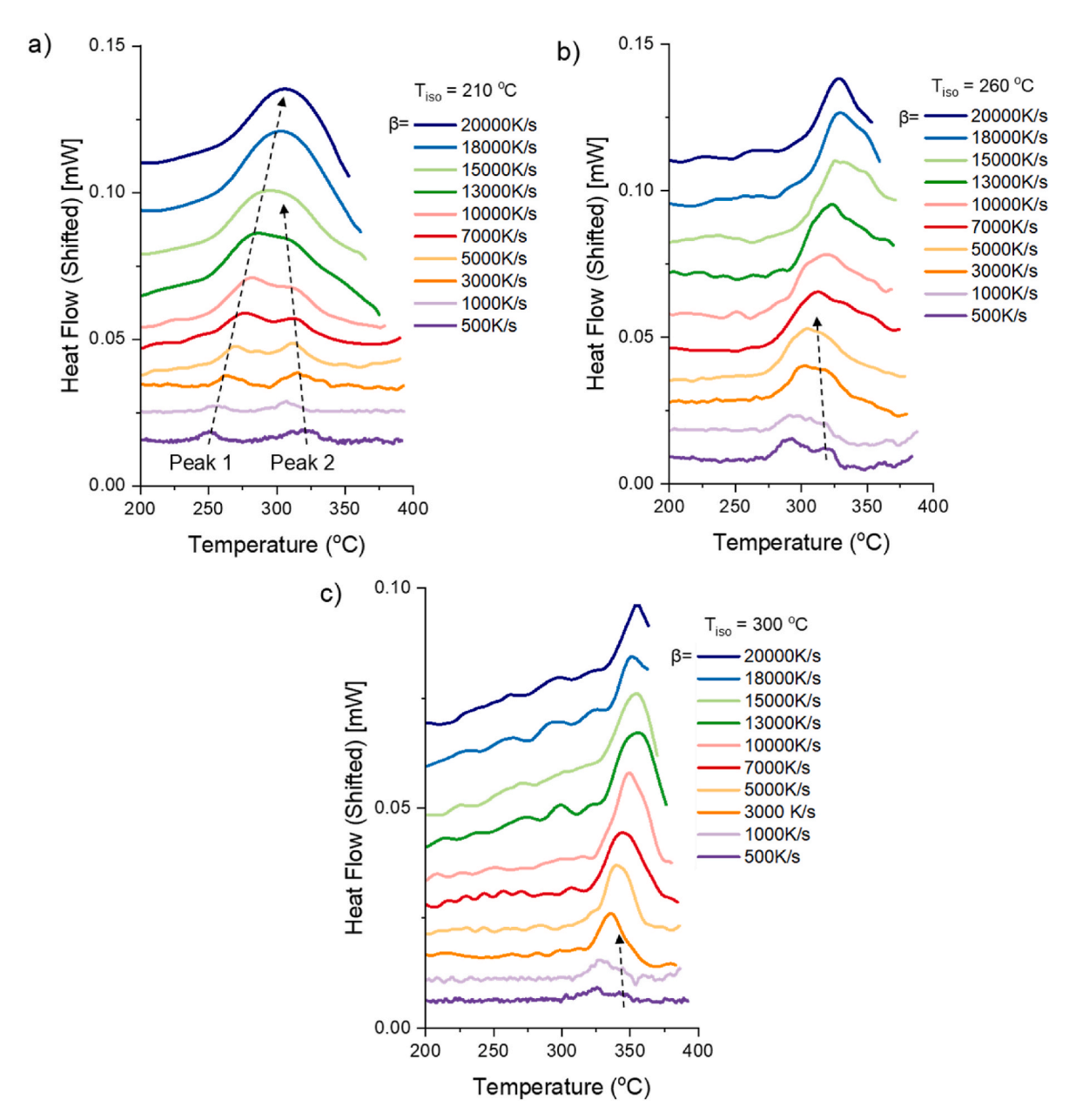


Fig. 7. Melting thermograms of PEKK 80/20 isothermally crystallized to low degrees of crystallinity at the indicated isothermal temperature and heated at the specified heating rate to observe suppression of melt reorganization. All thermograms were temperature corrected at each heating rate using an indium standard. Arrows indicate the shifting of peaks 1 and 2 with increasing heating rate.

Fig. 7 shows the FSC heating curves of PEKK 80/20 isothermally crystallized to low degrees of crystallization then heated from 500 K/s to 20,000 K/s. Multiple melting peak behavior is observed for all isothermal temperatures when heated at lower heating rates. Peak 1 shifts to higher temperature with increasing heating rate due to superheating. Superheating refers to the phenomenon where the heating rate is faster than the kinetics of melting of the polymer crystals and so the crystals appear to melt at a temperature above the size-dependent melting temperature [38]. As shown in Fig. 7a, Peak 2 shifts to slightly lower temperatures and then disappears above a certain critical heating rate (i.e., 18,000 K/s). In addition, Peak 2 disappears at a lower heating rate as  $T_{iso}$  is increased to 260 °C and 300 °C (Fig. 7b and c, respectively). These results indicate that Peak 2 is due to the melting of reorganized crystals during heating as the reorganization is suppressed within the time-limited conditions of the increased heating rate. The suppression of reorganization with lower heating rates at higher Tiso suggests formation of more stable crystals with increasing Tiso. This same behavior has been observed for several polymers including PA 6 [20], iPP [39], and PEEK [19].

The sample masses utilized in this study are sufficiently small (4 ng - 13 ng) and thus the broadening and shifting of the melting peak to higher temperatures is not expected to be attributed to thermal lag [5, 19,40-42]. To quantitatively demonstrate that the shifting and broadening of Peak 1 with increased heating rate is not due to thermal lag but due to superheating only, the heating rate dependence of the melting temperature of the superheated polymer crystals can be analyzed utilizing equation (3), developed by Schawe et al. and simplified by Toda et al. [43,44].

$$T_{m,peak} = T_{ZEP} + A\beta^{z} \quad with \ 0 < z \le 0.5$$
 [3]

In this analysis T<sub>m,peak</sub> is the peak melting temperature, T<sub>ZEP</sub> is the zero-entropy-production temperature, A is a constant,  $\beta$  is the heating rate, and z is an exponent which provides information regarding melting kinetics. Zero-entropy-production (ZEP) refers to melting of a metastable crystal of a distinct thickness at its stability limit, i.e. without reorganization or superheating [19,29]. A value of  $z \le 0.5$  indicates no thermal lag effects and z > 0.5 indicates reorganization, recrystallization, and thermal lag effects cannot be ruled out. As discussed in detail by Toda et al., the exponent z is related to the characteristic melt time of a crystallite upon heating, which describes the transient nature of the melting kinetics. The characteristic melt time represents the mean residence time in the state of superheating and influences the degree of shift of the peak melting temperature due to superheating. A value of z < 0.5 indicates that the interfacial free energy is low indicating no nucleation upon heating is occurring (i.e., the observed melting point is not affected by reorganization attributed to nucleation at the crystal-melt interface). 41 Fig. 8 shows that the relationship between T<sub>m</sub>.  $_{peak}$  and heating rate scales to a power  $\beta^z$  for Peak 1 where the z values  $\dot{}$ corresponding to the best linear fits to equation (3) for each temperature are shown. With z values < 0.5 and a sufficiently small sample size, it has been demonstrated that thermal lag is not affecting the peak melting temperature over the range of heating rates explored [19,29,44].

After establishing that the peak melting temperature is not influenced by thermal lag, the  $T_{ZEP}$  is obtained as the y-intercept from the linear extrapolation of the plot of  $T_{m,peak}$  versus  $\beta^z$  to a heating rate of zero (Fig. 8). Over the range of experimental isothermal crystallization temperatures, the  $T_{ZEP}$  is found to increase linearly with increasing  $T_{iso}$  (i.e., a Hoffman-Weeks plot, Fig. 9) [29,30]. The equilibrium melting temperature,  $T_m^o$ , is then obtained from the interception of the linear extrapolation of the  $T_{ZEP}$  to the  $T_m = T_c$  line [20,26–28]. Using this analysis, the  $T_m^o$  for PEKK 80/20 is determined to be 382 °C. It is important to note that this value of  $T_m^o$  is 14 °C higher than the previously reported literature value of 368 °C [4].

The extrapolated  $T_m^o$  over a range of heating rates was also explored by linear Hoffman-Weeks analysis of  $T_{m,peak}$  versus  $T_{iso}$  to compare to the value obtained by the  $T_{ZEP}$  versus  $T_{iso}$  extrapolation. Fig. 10 shows

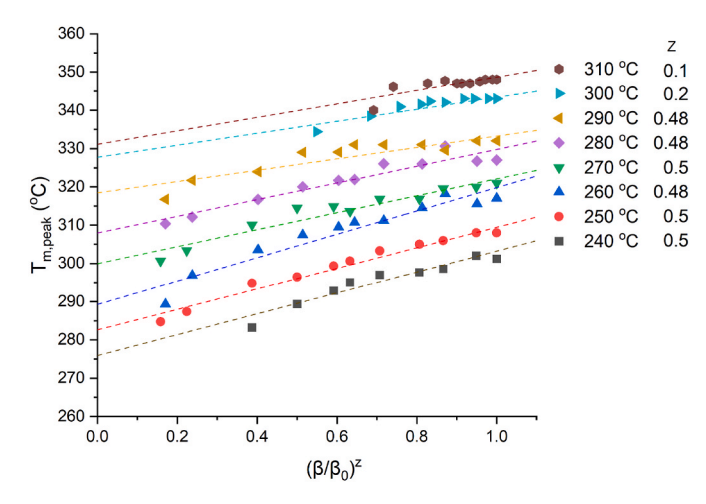


**Fig. 8.**  $T_{ZEP}$  analysis of PEKK 80/20 utilizing equation (3). Dashed lines indicate best linear fit and extrapolated to a heating rate of zero to indicate the  $T_{ZEP}$  value for each  $T_{iso}$ . The best fit values of the power z for each isothermal crystallization temperature are shown.

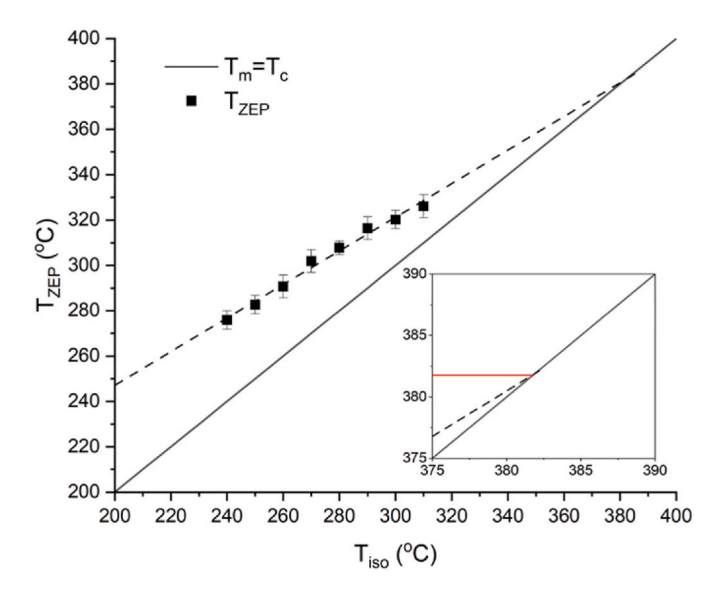
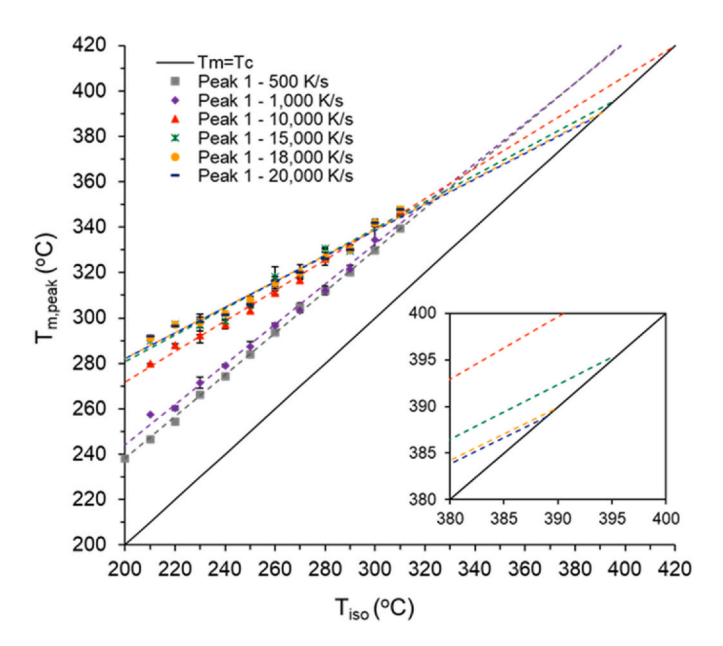


Fig. 9.  $T_{ZEP}$  versus  $T_{iso}$  Hoffman-Weeks extrapolation to  $T_{ZEP} = T_c$ . Inset highlights the point of intersection and extrapolation to  $T_m^o$  (red line).

the Hoffman-Weeks plot of peak melting temperatures, T<sub>m,peak</sub>, versus Tiso over a range of increasing heating rates. With increasing heating rate, the slope of the Hoffman-Weeks plots decreases. As discussed previously, this behavior is explained by more stable crystals forming at higher isothermal crystallization temperatures, thus reducing the ability to reorganize, resulting in lower heating rates required to suppress reorganization. For each heating rate, the T<sub>m</sub><sup>0</sup> is extrapolated from the interception of the linear extrapolation of the peak melting temperatures to the T<sub>m</sub>=T<sub>c</sub> line. With increasing heating rate, the extrapolated intersection with T<sub>m</sub>=T<sub>c</sub> line decreases due to the inhibition of reorganization of crystallites. At sufficiently fast heating rates (to prevent reorganization or thickening of crystallites), the extrapolated plots converge to a relatively constant value of  $T_m^0 = 388$  °C. Through this analysis, it is now clear that a heating rate of 18,000 K/s is sufficiently fast enough to arrest all melt-reorganization. Therefore, in the absence of melt-reorganization or crystal thickening, the T<sub>m</sub> of PEKK 80/20 by this traditional Hoffman-Weeks extrapolation is noted to be 6 °C higher than the  $T_{ZEP}$  versus  $T_{iso}$  determined value of 382  $^{\circ}\text{C}.$  Since the  $T_{ZEP}$ method 1 considers only the equilibrium melting phenomenon i.e., in



**Fig. 10.** The Hoffman-Weeks plot of PEKK 80/20. Increasing heating rates suppress reorganization of crystallites and result in a lower equilibrium melting temperature. Peak melting temperature was determined by deconvolution of melting peaks from indium corrected melting profiles.

the absence of heating rate dependence, the 6  $^{\circ}\text{C}$  increase in the extrapolated  $T_{0}^{\text{m}}$  value for method 2 is attributed to superheating.

# 4. Conclusions

Fast scanning calorimetry (FSC) is necessary to study the crystallization kinetics and determine the T<sub>m</sub> of fast crystallizing PEKK 80/20. The linear topology and comonomer composition are confirmed by <sup>1</sup>H and <sup>13</sup>C NMR. The crystallization half-time of PEKK 80/20 exhibits parabolic behavior with the most rapid crystallization ( $t_{1/2} = 12$  s) occurring at 260 °C. Furthermore, thorough analysis of the origins of the multiple melting peak behavior of PEKK 80/20 demonstrated that the multiple melting peaks are due to melt-reorganization upon heating at insufficient rates and not due to a bimodal distribution of crystal sizes with district melting temperatures. Over a wide range of experimental isothermal crystallization temperatures, the zero entropy production temperature, T<sub>ZEP</sub>, was found to increase linearly with increasing T<sub>iso</sub>, and extrapolation to the  $T_m = T_c$  line yielded an accurate determination of  $T_m^0 = 382$  °C for the commercially-available KEPSTAN PEKK 8001 (T/ I=80/20). This refined equilibrium melting temperature for PEKK 80/ 20 is significantly greater than the widely cited value obtained from an experimental grade of PEKK using conventional DSC. As a further comparison, a conventional Hoffman-Weeks analysis was performed with FSC at heating rates sufficient to arrest melt-reorganization (i.e., heating rates greater than 18,000 K/s). This analysis yielded a T<sub>m</sub> value that was just 6  $^{\circ}\text{C}$  higher than the  $T_{ZEP}$  method. While both FSC methods showed reasonably good agreement, the somewhat higher T<sub>m</sub> value from the conventional Hoffman-Weeks extrapolation was attributed to unavoidable effects of superheating at fast scan rates.

# CRediT authorship contribution statement

**Michelle E. Pomatto:** Conceptualization, Data curation, Formal analysis, Investigation, Methodology, Writing – original draft, Writing – review & editing. **Robert B. Moore:** Conceptualization, Funding acquisition, Project administration, Supervision, Writing – review & editing.

#### **Declaration of competing interest**

The authors declare the following financial interests/personal relationships which may be considered as potential competing interests:  $\frac{1}{2} \int_{-\infty}^{\infty} \frac{1}{2} \left( \frac{1}{2} \int_{-\infty}^{\infty}$ 

Robert B. Moore reports financial support was provided by National Science Foundation.

#### Data availability

Data will be made available on request.

# Acknowledgements

The authors thank Arkema for providing KEPSTAN 8001 and KEPSTAN 7002 samples used for this work as well as the Virginia Tech Chemistry Department for laboratory support. This work was supported by the National Science Foundation under grant No. DMR-1809291 and DMR-2104856.

# Appendix A. Supplementary data

Supplementary data to this article can be found online at https://doi.org/10.1016/j.polymer.2023.125810.

#### References

- L. Quiroga Cortés, N. Caussé, E. Dantras, A. Lonjon, C. Lacabanne, Morphology and dynamical mechanical properties of poly ether ketone ketone (PEKK) with meta phenyl links, J. Appl. Polym. Sci. 133 (19) (2016).
- [2] M. Reitman, D. Jaekel, R. Siskey, S.M. Kurtz, Chapter 4 morphology and crystalline architecture of polyaryletherketones, in: S.M. Kurtz (Ed.), PEEK Biomaterials Handbook, William Andrew Publishing, Oxford, 2012, pp. 49–60.
- [3] S.Z.D. Cheng, R.-M. Ho, B.S. Hsiao, K.H. Gardner, Polymorphism and crystal structure identification in poly(aryl ether ketone ketone)s, Macromol. Chem. Phys. 197 (1) (1996) 185–213.
- [4] K.H. Gardner, B.S. Hsiao, R.R. Matheson, B.A. Wood, Structure, crystallization and morphology of poly (aryl ether ketone ketone), Polymer 33 (12) (1992) 2483–2495.
- [5] B.S. Hsiao, K.H. Gardner, S.Z.D. Cheng, Crystallization of poly(aryl ether ketone ketone) copolymers containing terephthalate/isophthalate moieties, J. Polym. Sci. B Polym. Phys. 32 (16) (1994) 2585–2594.
- [6] P.J. Holdsworth, A. Turner-Jones, The melting behaviour of heat crystallized poly (ethylene terephthalate), Polymer 12 (3) (1971) 195–208.
- [7] A.A. Minakov, D.A. Mordvintsev, C. Schick, Melting and reorganization of poly (ethylene terephthalate) on fast heating (1000 K/s), Polymer 45 (11) (2004) 2755–2763
- [8] A.A. Minakov, D.A. Mordvintsev, R. Tol, C. Schick, Melting and reorganization of the crystalline fraction and relaxation of the rigid amorphous fraction of isotactic polystyrene on fast heating (30,000K/min), Thermochim. Acta 442 (1) (2006) 25, 30
- [9] S. Sohn, A. Alizadeh, H. Marand, On the multiple melting behavior of bisphenol-A polycarbonate, Polymer 41 (25) (2000) 8879–8886.
- [10] A. Alizadeh, L. Richardson, J. Xu, S. McCartney, H. Marand, Y.W. Cheung, S. Chum, Influence of structural and topological constraints on the crystallization and melting behavior of polymers. 1. Ethylene/1-Octene copolymers, Macromolecules 32 (19) (1999) 6221–6235.
- [11] H. Marand, A. Alizadeh, R. Farmer, R. Desai, V. Velikov, Influence of structural and topological constraints on the crystallization and melting behavior of polymers. 2. Poly(arylene ether ether ketone), Macromolecules 33 (9) (2000) 3392–3403.
- [12] P. Cebe, S.-D. Hong, Crystallization behaviour of poly(ether-ether-ketone), Polymer 27 (8) (1986) 1183–1192.
- [13] D.J. Blundell, On the interpretation of multiple melting peaks in poly(ether ether ketone), Polymer 28 (13) (1987) 2248–2251.
- [14] S.Z. Cheng, M. Cao, B. Wunderlich, Glass transition and melting behavior of poly (oxy-1, 4-phenyleneoxy-1, 4-phenylenecarbonyl-1, 4-phenylene)(PEEK), Macromolecules 19 (7) (1986) 1868–1876.
- [15] R.-M. Ho, S.Z.D. Cheng, B.S. Hsiao, K.H. Gardner, Crystal morphology and phase identification in poly(aryl ether ketone)s and their copolymers. 3. Polymorphism in a polymer containing alternated terephthalic acid and isophthalic acid isomers, Macromolecules 28 (6) (1995) 1938–1945.
- [16] A.G. Al Lafi, G. Alsayes, Interpretation of multiple melting behaviour in poly (ether ether ketone) revisited: two-dimensional correlation mapping approach, J. Therm. Anal. Calorim. (2021) 1–8.
- [17] T. Choupin, B. Fayolle, G. Régnier, C. Paris, J. Cinquin, B. Brulé, Isothermal crystallization kinetic modeling of poly(etherketoneketone) (PEKK) copolymer, Polymer 111 (2017) 73–82.
- [18] K.H. Gardner, B.S. Hsiao, K.L. Faron, Polymorphism in poly(aryl ether ketone)s, Polymer `35 (11) (1994) 2290–2295.

- [19] Y. Furushima, A. Toda, V. Rousseaux, C. Bailly, E. Zhuravlev, C. Schick, Quantitative understanding of two distinct melting kinetics of an isothermally crystallized poly (ether ether ketone), Polymer 99 (2016) 97–104.
- [20] Y. Furushima, M. Nakada, K. Ishikiriyama, A. Toda, R. Androsch, E. Zhuravlev, C. Schick, Two crystal populations with different melting/reorganization kinetics of isothermally crystallized polyamide 6, J. Polym. Sci. B Polym. Phys. 54 (20) (2016) 2126–2138.
- [21] X. Tardif, B. Pignon, N. Boyard, J.W.P. Schmelzer, V. Sobotka, D. Delaunay, C. Schick, Experimental study of crystallization of PolyEtherEtherKetone (PEEK) over a large temperature range using a nano-calorimeter, Polym. Test. 36 (2014) 10–19.
- [22] R. Verma, H. Marand, B. Hsiao, Morphological changes during secondary crystallization and subsequent melting in poly(ether ether ketone) as studied by real time small angle X-ray scattering, Macromolecules 29 (24) (1996) 7767–7775
- [23] S. Tencé-Girault, J. Quibel, A. Cherri, S. Roland, B. Fayolle, S. Bizet, I. Iliopoulos, Quantitative structural study of cold-crystallized PEKK, ACS Applied Polymer Materials 3 (4) (2021) 1795–1808.
- [24] H. Pérez-Martín, P. Mackenzie, A. Baidak, C.M. Ó Brádaigh, D. Ray, Crystallinity studies of PEKK and carbon fibre/PEKK composites: a review, Compos. B Eng. 223 (2021) 109127
- [25] H. Marand, Z. Huang, Isothermal lamellar thickening in linear polyethylene: correlation between the evolution of the degree of crystallinity and the melting temperature, Macromolecules 37 (17) (2004) 6492–6497.
- [26] R. Zhang, K. Jariyavidyanont, E. Zhuravlev, C. Schick, R. Androsch, Zero-entropy-production melting temperature of crystals of poly(butylene succinate) formed at high supercooling of the melt, Macromolecules 55 (3) (2022) 965–970.
- [27] A. Toda, K. Taguchi, K. Nozaki, M. Konishi, Melting behaviors of polyethylene crystals: an application of fast-scan DSC, Polymer 55 (14) (2014) 3186–3194.
- [28] A. Toda, K. Taguchi, G. Kono, K. Nozaki, Crystallization and melting behaviors of poly(vinylidene fluoride) examined by fast-scan calorimetry: Hoffman-Weeks, Gibbs-Thomson and thermal Gibbs-Thomson plots, Polymer 169 (2019) 11–20.
- [29] B. Wunderlich, Crystal Melting, Macroscopic Physics, Academic Press, New York,
- [30] J.D. Hoffman, G.T. Davis, J.I. Lauritzen, The Rate of Crystallization of Linear Polymers with Chain Folding, Springer, US, 1976, pp. 497–614.
- [31] H. Marand, J. Xu, S. Srinivas, Determination of the equilibrium melting temperature of polymer crystals: linear and nonlinear Hoffman—Weeks extrapolations, Macromolecules 31 (23) (1998) 8219–8229.

[32] R.G. Alamo, B.D. Viers, L. Mandelkern, A re-examination of the relation between the melting temperature and the crystallization temperature: linear polyethylene, Macromolecules 28 (9) (1995) 3205–3213.

Polymer 271 (2023) 125810

- [33] L.J. Anderson, X. Yuan, G.B. Fahs, R.B. Moore, Blocky ionomers via sulfonation of poly(ether ether ketone) in the semicrystalline gel state, Macromolecules 51 (16) (2018) 6226–6237.
- [34] J. Seo, A.M. Gohn, O. Dubin, H. Takahashi, H. Hasegawa, R. Sato, A.M. Rhoades, R. P. Schaake, R.H. Colby, Isothermal crystallization of poly(ether ether ketone) with different molecular weights over a wide temperature range, POLYMER CRYSTALLIZATION 2 (1) (2019).
- [35] S.J. Talley, C.L. AndersonSchoepe, C.J. Berger, K.A. Leary, S.A. Snyder, R.B. Moore, Mechanically robust and superhydrophobic aerogels of poly(ether ether ketone), Polymer 126 (2017) 437–445.
- [36] W. Vogel, M. Hegde, A.N. Keith, S.S. Sheiko, T.J. Dingemans, Chemistry and properties of cross-linked all-aromatic hyperbranched polyaryletherketones, Macromolecules 55 (1) (2022) 100–112.
- [37] T. Choupin, B. Fayolle, G. Régnier, C. Paris, J. Cinquin, B. Brulé, A more reliable DSC-based methodology to study crystallization kinetics: application to poly(ether ketone ketone) (PEKK) copolymers, Polymer 155 (2018) 109–115.
- [38] H. Gao, J. Wang, C. Schick, A. Toda, D. Zhou, W. Hu, Combining fast-scan chipcalorimeter with molecular simulations to investigate superheating behaviors of lamellar polymer crystals, Polymer 55 (16) (2014) 4307–4312.
- [39] J.E.K. Schawe, Analysis of non-isothermal crystallization during cooling and reorganization during heating of isotactic polypropylene by fast scanning DSC, Thermochim. Acta 603 (2015) 85–93.
- [40] A. Toda, M. Konishi, An evaluation of thermal lags of fast-scan microchip DSC with polymer film samples, Thermochim. Acta 589 (2014) 262–269.
- [41] A. Toda, Heating rate dependence of melting peak temperature examined by DSC of heat flux type, J. Therm. Anal. Calorim. 123 (3) (2016) 1795–1808.
- [42] A. Toda, K. Taguchi, K. Sato, K. Nozaki, M. Maruyama, K. Tagashira, M. Konishi, Melting kinetics of it-polypropylene crystals over wide heating rates, J. Therm. Anal. Calorim. 113 (3) (2013) 1231–1237.
- [43] J.E.K. Schawe, G.R. Strobl, Superheating effects during the melting of crystallites of syndiotactic polypropylene analysed by temperature-modulated differential scanning calorimetry, Polymer 39 (16) (1998) 3745–3751.
- [44] A. Toda, M. Hikosaka, K. Yamada, Superheating of the melting kinetics in polymer crystals: a possible nucleation mechanism, Polymer 43 (5) (2002) 1667–1679.